

# EVALUATION OF OPTIMAL MODEL FOLLOWING CONTROLLERS IN TERMS OF HANDLING QUALITIES

Ilgaz Doga Okcu  
iokcu@tai.com.tr  
Design Engineer

Umut Ture  
umut.ture@tai.com.tr  
Design Engineer

Turkish Aerospace Industries, Inc.  
Ankara, Turkey

## Abstract

This work describes four different optimal model following controller synthesis for helicopter control near hovering flight and comparisons of these controllers especially in terms of handling qualities (HQ) in light of ADS-33E-PRF guidelines. A nonlinear mathematical model representing Bell 206B dynamics constructed in FLIGHTLAB environment. A basic linear reference model is formulated in light of the handling qualities specifications. The same reference model is used for all model following controllers. The response type is attitude-command-attitude-hold (ACAH) for pitch, roll and yaw axes where heave axis has a rate command augmentation. The mathematical bases for the controller are given. Tracking performance results for hover flight condition are presented. The ability of the controllers to mimic the reference model in terms of applicable handling qualities specifications is assessed with the help of CONDUIT<sup>®</sup>. An optimization effort for the weighings of the optimal controllers is carried out to achieve level 1 handling qualities, notable results are presented.

## 1 INTRODUCTION

It is a known and emphasized fact that having good HQ characteristics results in reduced pilot work-load, increased safety, high mission performance and reduce the cost and development process for new designs<sup>[1]</sup>. With the introduction of ADS-33, flight control engineers of today knows a great deal about how a rotorcraft with Level 1 HQ rating should behave. The major challenge of flight control is mainly reduced to coming up with the design that meets these requirements and to retrofit existing aircraft with control augmentation systems that ensures Level 1 handling<sup>[2]</sup>.

The model following control concept provides the flight control engineer the ability to include performance requirements in to the control synthesis<sup>[3]</sup>. In situations where a design standard is available, MFC is the natural choice. This practicality led MFC to be used extensively in the helicopter flight control applications over the years<sup>[4;5;6]</sup>. MFC is well suited for use with the optimal control theory. Utilizing the optimal feedback gains for MFC is a widely used, simple, flexible method<sup>[7]</sup>. However, optimal MFC framework suffers from one major disadvantage: the weighing of the cost function. Weight determination for the states and inputs of the system is generally a timely and trial-and-error based process.

CONDUIT<sup>®</sup> is a multi-objective parametric optimization tool that can be used to find suitable design parameters of a given control architecture based on the HQ specifications selected by the user<sup>[1]</sup>. The flexibility of the MFC introduced by the variable weighing matrix elements can be used in conjunction with CONDUIT<sup>®</sup>, eliminating the disadvantage

caused by the uncertainty associated with the weighing matrices.

In this paper, four different optimal model following controllers are devised for the hovering flight of Bell 206B helicopter. A reference model is constructed based on the HQ requirements<sup>[8]</sup>. Time response analyses were completed to find the initial weighings and CONDUIT<sup>®</sup> based optimization is performed where MFC falls short in terms of HQ ratings. To achieve compatibility with different controllers, reference model parameters are not included in the design parameters at the optimization stage. This way all of the controllers are compared against the same reference model, revealing their shortcomings or strengths based solely on the control algorithm itself.

Selected control types all serve the same purpose; however, each with different approach. In implicit model following control (IMF), the aim is to minimize the error between the derivatives of the plant and reference model, thus forcing closed loop systems roots to be identical to reference model's. Reference model is only used in the quadratic performance index in IMF. Explicit model following, on the other hand, uses reference model as a part of the control architecture. Widely used command generator tracker (CGT) method is adapted as well as reference feed-forward (RFF) technique to convert an ordinarily tracking problem in to a regulator problem. The last method uses plant inverse in the feed-forward path with the reference model and referred to as model inversion (MI) explicit model following in this paper.

## 2 BELL 206B MODELING

The platform used in this research is the Bell 206B Je-tranger helicopter. Bell 206B is a classical configuration medium sized utility helicopter. The main rotor of the helicopter has a teetering, under-slung structure. TAI has a Bell 206B helicopter in its possession for research and development purposes. FLIGHTLAB is selected as the modeling tool for constructing the flight dynamics model<sup>[9]</sup>. Necessary helicopter parameters for modeling were gathered from flight manual, measurements and weighings conducted on the helicopter at TAI facilities. Result is a high fidelity non linear simulation model of Bell 206B helicopter with real time computational capacity suitable for piloted simulations. The full nonlinear model has 31 states to define dynamics including rigid body dynamics, rotor dynamics and control system dynamics.

Reduced 9 state linear models, including the rigid body helicopter dynamics, obtained from the FLIGHTLAB are used in control synthesis. The linearization is based on steady hovering flight for which the helicopter exhibits unstable modes. 1 gives the state space representation of reduced order model for Bell 206B.

$$(1) \quad \dot{x}(t) = Ax(t) + Bu(t), \quad x = \begin{bmatrix} \phi \\ \theta \\ \psi \\ u \\ v \\ w \\ p \\ q \\ r \end{bmatrix}, \quad u = \begin{bmatrix} \delta_{lon} \\ \delta_{lat} \\ \delta_{col} \\ \delta_{ped} \end{bmatrix}$$

Where  $x(t) \in \mathbb{R}^{9 \times 1}$  is the state vector and  $u(t) \in \mathbb{R}^{4 \times 1}$  is the input vector to the linear helicopter model.

The actuators of the Bell 206 are modeled as first order transfer functions with 12 Hertz bandwidth. A 2ms delay is added to the closed loop system to account for computations. The sensor dynamics are represented as second order transfer functions with a 5 Hertz frequency and 0.7 damping ratio.

The mathematical model trim results are verified with the flight tests performed by TAI.

## 3 CONTROL SYSTEM DESIGN

All control techniques in this study uses a  $H_2$  minimization to come up with a controller to superpose the frequency responses of the reference model and the actual plant. Linear quadratic regulator as developed by Tyler supplies a closed loop solution for a stable, optimal system according to weighings selected by the designer<sup>[10]</sup>. Techniques differ in terms of problem formulation but all has optimal control theory in the core of the synthesis and serve the same purpose of stabilizing the helicopter and shaping its response similar to reference model.

It is suitable to define a performance output list out of the plant and reference model states,  $z(t) \in \mathbb{R}^{4 \times 1}$ ,

$$(2) \quad z(t) = Hx(t) = \begin{bmatrix} \phi \\ \theta \\ \psi \\ r \end{bmatrix} \quad z_m(t) = Hx_m(t) = \begin{bmatrix} \phi_m \\ \theta_m \\ \psi_m \\ r_m \end{bmatrix}$$

With  $H \in \mathbb{R}^{4 \times 9}$  is the performance index matrix. The performance output list consists of suitable states for ACAH and RCHH response types.

### 3.1 Reference Model

A reference model representing the desired closed loop performance is constructed according to standard rotorcraft handling qualities specifications found in ADS-33e-PRF<sup>[8]</sup>. The strategy for constructing the model is based on first identifying transfer functions for each axis and then incorporating them all into a state space system<sup>[7]</sup>.

Reference model is constructed in such a way that, a unit command in pitch, roll and yaw axes will result in a unit attitude change (ACAH) and a unit step command in heave will result in a rate response (RCHH). The reference model has no inherit cross-coupling and has the same states as the reduced 9 state linear models. Pitch, roll and yaw axis responses are second order and collective response is a first order transfer function with appropriate time constants. Damping ratio and natural frequency of the second order transfer functions and time constants of the first order transfer functions exceed the requirements of the handling qualities specifications since perfect model following may not be achieved. State space reference model is given in 3.

$$(3) \quad \dot{x}_m(t) = A_m x_m(t) + B_m r(t)$$

$x_m(t) \in \mathbb{R}^{9 \times 1}$  is the reference model state vector and  $r(t) \in \mathbb{R}^{4 \times 1}$  is the reference input vector containing pitch and roll attitudes, yaw rate, and vertical velocity commands. The state and control matrices of the reference model are denoted by  $A_m, B_m$ .

### 3.2 Command Generator Tracker MFC

The command generator tracker technique is used to convert the classical linear quadratic regulator problem in to a tracking problem<sup>[3]</sup>. The error signal to be regulated is  $e(t) \in \mathbb{R}^{4 \times 1}$ ,

$$(4) \quad e(t) = z_m(t) - z(t) = Hx_m(t) - Hx(t) = \begin{bmatrix} \phi_e \\ \theta_e \\ \psi_e \\ r_e \end{bmatrix}$$

Collecting the plant and reference model dynamics into one augmented system yields

$$(5) \quad \begin{bmatrix} \dot{x} \\ \dot{x}_m \end{bmatrix} = \begin{bmatrix} A & 0 \\ 0 & A_m \end{bmatrix} \begin{bmatrix} x \\ x_m \end{bmatrix} + \begin{bmatrix} B \\ 0 \end{bmatrix} u + \begin{bmatrix} 0 \\ B_m \end{bmatrix} r$$

$$\dot{x}'(t) = A'x'(t) + B'u(t) + G'r(t), x' = \begin{bmatrix} x \\ x_m \end{bmatrix}$$

It is now appropriate to use a command generator to obtain a regulator problem instead of a tracking (servo) problem. The command generator can be thought as an additional system in front of the actual plant, that has no input signals but all the required initial conditions to output the reference signal for the actual plant. These kind of systems satisfy the differential equation defined by the  $\delta$  operator

$$(6) \quad \Delta(m) = m^{(d)} + a_{d-1}m^{(d-1)} + \dots + a_1m = 0$$

Many reference signals of interest indeed satisfy 6. For example a unit step input has  $\dot{r} = 0$  and  $r(0) = r_0$  corresponding to  $d = 1$  and  $a_d = 0$  in 6. Applying the  $\delta$  operator to 5 removes the reference signal input from the system since it satisfies the command generator equation.

$$(7) \quad \dot{\xi}(t) = A'\xi(t) + B'\mu(t)$$

The modified states and control variables are

$$(8) \quad \xi(t) = \Delta(x'(t)) = x'(t) = \begin{bmatrix} \xi_p(t) \\ \xi_m(t) \end{bmatrix}$$

$$\mu(t) = \Delta(u(t)) = \dot{u}(t)$$

The subscripts  $p$  and  $m$  denote the plant and reference model states respectively. It is now adequate to introduce error states to the system. Applying 6 on the error defined in 4 results in

$$(9) \quad \Delta(e(t)) = \dot{e}(t) = [-H \quad H] \xi(t) = H'\xi(t)$$

Collecting 7 and 9 together

$$(10) \quad \begin{bmatrix} \dot{e}(t) \\ \dot{\xi}(t) \end{bmatrix} = \begin{bmatrix} 0 & H' \\ 0 & A' \end{bmatrix} \begin{bmatrix} e(t) \\ \xi(t) \end{bmatrix} + \begin{bmatrix} 0 \\ B' \end{bmatrix} \mu(t)$$

Using 10 it is possible to obtain a full-state feedback gain to regulate the systems states and error to zero. It is obvious from 4 if  $e(t)$  goes zero the plant will follow the selected reference model states. With error signals included in the states of 10, proper modification of the state weighing matrix,  $\hat{Q}$ , in the optimal cost function will allow penalizing  $e(t)$ . Error signal in terms of states is

$$(11) \quad e(t) = [I_4 \quad 0_{4 \times 16}] \xi'(t) = C_e \xi'(t)$$

that leads to the modified state weighing matrix

$$(12) \quad \tilde{Q} = C_e^T Q C_e$$

Optimal cost function for the system

$$(13) \quad J = \frac{1}{2} \int_0^\infty \xi'^T(t) \tilde{Q} \xi'(t) + \mu^T(t) R \mu(t) dt$$

resulting in the control law

$$(14) \quad \mu(t) = -K_e e(t) - K_p \xi_p(t) - K_m \xi_m(t)$$

$$K = [K_e \quad K_p \quad K_m]$$

Integrating to obtain input signal  $u(t)$

$$(15) \quad u(t) = \int \mu dt = -K_e \int e(t) dt - K_p x(t) - K_m x_m(t)$$

The final control law consists of a feed-forward and a feedback path and an additional integral controller on the error channel very much like the popular LQI control. With the reference model states included in the control system, CGT control law guarantees asymptotic tracking. The block diagram of the controller is illustrated in Figure 1.

### 3.3 Reference Feed Forward MFC

Another way to handle the tracking problem of hovering helicopter flight by LQR theory is presented in<sup>[7]</sup>. Reference feed forward (RFF) explicit model following design is based on the assumption that the reference signal  $r(t)$  is dependent on the system error defined in 4.

$$(16) \quad \dot{r}(t) = Lr(t) + e(t) = Lr(t) - Hx(t) + Hx_m(t)$$

16 can be interpreted as a basic pilot model. For a diagonal matrix  $L$ , expanding the equation reveals first order transfer functions that takes the corresponding error signal as input and generates a correction on the appropriate command channel with a specified time constant. For simplicity it is assumed that there is no lag between the error generation and pilot reaction, and all elements of  $L$  are taken as zero.

Combining 1, 3, and 16 yields an open loop system suitable for full-state optimal control.

$$(17) \quad \begin{bmatrix} \dot{x} \\ \dot{x}_m \\ \dot{r} \end{bmatrix} = \begin{bmatrix} A & 0 & 0 \\ 0 & A_m & B_m \\ -H & H & L \end{bmatrix} \begin{bmatrix} x \\ x_m \\ r \end{bmatrix} + \begin{bmatrix} B \\ 0 \\ 0 \end{bmatrix} u$$

$$\hat{x}(t) = \hat{A}\hat{x}(t) + \hat{B}\hat{u}(t), \hat{x}(t) = \begin{bmatrix} x \\ x_m \\ r \end{bmatrix}$$

Again proper modification of the state weighing matrix  $\hat{Q}$  is required to penalize error signals. Optimal cost function to be minimized is

$$(18) \quad J = \frac{1}{2} \int_0^{\infty} \dot{x}^T(t) \hat{Q} \dot{x}(t) + u^T(t) R u(t) dt$$

$$\hat{Q} = \begin{bmatrix} H^T Q H & -H^T Q H & 0 \\ -H^T Q H & H^T Q H & 0 \\ 0 & 0 & 0 \end{bmatrix}$$

Resulting control law is very similar that of 15 technique. Only addition is the initial reference signal,  $r(0)$  as a feed-forward compensator. Equation 19 also guarantees asymptotic tracking. The block diagram of the controller is illustrated in Figure 1.

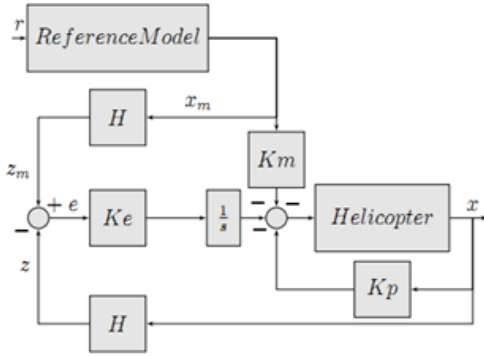


Figure 1: CGT and RFF Controller Block Diagram

$$(19) \quad u(t) = -K_p x(t) - K_m x_m(t) - K_r \int e(t) dt + K_r r(0)$$

### 3.4 Implicit MFC

IMF technique uses feedback and feed-forward compensation in attempt to match the dynamics of the controlled plant to reference model dynamics. Matching of the dynamics are achieved by adjusting the pole locations of the closed loop system. IMF forces the plant to be the reference model. IMF design for aircraft flight control is well defined in [7;10;11].

$$(20) \quad u(t) = Kx(t) + Fr(t) = u_{fb} + u_{ff}$$

The aim is to acquire the feed-forward and feedback matrices  $F$  and  $K$  that will force the plant to follow pilot inputs. The reference model for IMF control law is

$$(21) \quad \dot{x}(t) = A_m x(t)$$

In general, perfect following for the ideal model with no input will not hold and a model following error,  $e(t)$ , will occur. The error is defined as the difference between the derivative of the states rather than states themselves. Using 1 and 21

$$(22) \quad e(t) = \dot{x}(t) - A_m x(t) = (A - A_m)x(t) + B u(t)$$

Cost function is constructed in light of 22 as

$$(23) \quad J = \frac{1}{2} \int_0^{\infty} e^T(t) Q e(t) + u^T(t) R u(t) dt$$

$$= \frac{1}{2} \int_0^{\infty} x^T(t) \hat{Q} x(t) + 2x^T(t) \hat{S} u(t) + u^T(t) \hat{R} u(t) dt$$

With the matrix relations given in 24 the minimization of 23 reduces to algebraic Riccati equation given in 25.

$$(24) \quad \hat{Q} = (A - A_m)^T Q (A - A_m)$$

$$\hat{S} = (A - A_m)^T Q B$$

$$\hat{R} = R + B^T Q B$$

$$(25) \quad P \hat{A} + \hat{A}^T P - P B \hat{R}^{-1} B^T P + Q^* = 0$$

$$Q^* = \hat{Q} - \hat{S} \hat{R}^{-1} \hat{S}^T$$

$$\hat{A} = A - B \hat{R}^{-1} \hat{S}^T$$

Resulting gain matrices as given by [11] are defined as;

$$(26) \quad u_{fb}(t) = Kx(t) = \hat{R}^{-1} (B^T P + \hat{S}^T) x(t)$$

$$u_{ff}(t) = Fr(t) = \hat{R}^{-1} B^T (A + BK)^{-T} A_m^T Q B_m r(t)$$

The block diagram of the controller is illustrated in Figure 2.

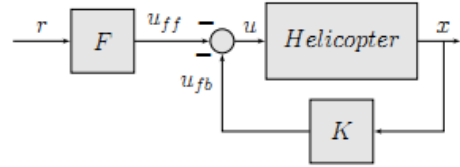


Figure 2: IMF Controller Block Diagram

### 3.5 Model Inversion MFC

The MI controller technique is adapted from [4]. Pilot inputs are fed through the reference model to obtain desired aircraft states and their derivatives. The derivatives are needed for the inverted model used in the feed-forward path of the controller. A feedback part is used to stabilize the naturally unstable helicopter model. The feedback part of the design is independent of the reference model or inverse model and can be designed by any control technique desired. In sake of comparison, the feedback part is designed using LQR theory in this work.

The assumed control is given as

$$(27) \quad u(t) = \underbrace{F x_m(t)}_{u_{ff}(t)} + \underbrace{K(x_m(t) - x(t))}_{u_{fb}(t)}$$

The feed-forward part has the pseudo-inverse model denoted by  $B^\dagger \in \mathbb{R}^{4 \times 9}$ .

$$(28) \quad u(t) = B^\dagger(\dot{x}_m - Ax_m) + K(x_m - x)$$

The error of the MI model following control law is defined as the error between plant and reference model states.

$$(29) \quad \begin{aligned} e &= x_m - x \\ \dot{e} &= \dot{x}_m - \dot{x} = A_m x_m + B_m r - Ax - Bu \end{aligned}$$

Substituting 28 into 29 and rearranging the equation using 3 yields

$$(30) \quad \begin{aligned} \dot{e} &= A_m x_m + B_m r - Ax - B[B^\dagger(\dot{x}_m - Ax_m) + K(x_m - x)] \\ \dot{e} &= (A - BK)(x_m - x) = (A - BK)e \end{aligned}$$

Equation 30 states that, the error dynamics of the MI control law is governed by the closed loop system  $(A - BK)$ . That is, if the feedback matrix  $K$  is chosen such that the eigenvalues of the  $(A - BK)$  are all negative, error signals will eventually go to zero. LQR design is used similar to RFF case to regulate the error dynamics of MI controller.

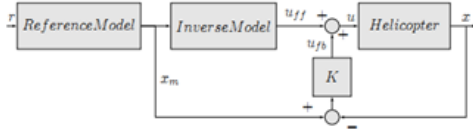


Figure 3: MI Controller Block Diagram

## 4 PARAMETER OPTIMIZATION

For a optimization problem setup in CONDUIT<sup>®</sup>, at least two main aspects need to be specified: the design parameters to be optimized and the HQ specifications to be optimized against. As mentioned earlier, it is reasonable to choose the diagonal weighing matrix elements as design parameters for the optimization process of an LQ controller in CONDUIT<sup>®</sup> environment. This way, the designer's influence on the controllers will be mostly removed and the most applicable approach in terms of HQ ratings could be discovered. At this point it is important to note that, non-diagonal weighing matrices can also be experimented with and may lead to better solutions; however, one of the main concerns during this work was to keep the design parameters as minimum as possible without losing the physical aspect of the problem. This same concern is the reason for not separating the feed forward and feedback parts of MI controller. It is really unfair to compare a controller that has considerably more design parameters than another, since it would have much more flexibility.

Table 1: Optimization Specification Set

Description	Type	Comments
Damping Ratio (Generic)	H	Ensures sufficient damping
Eigenvalues	H	Ensure Stability
Robust Stability	H	Ensure robust stability
Bandwidth (Pitch&Roll)	S	Short term pitch roll response requirement
Bandwidth (Yaw)	S	Short term yaw response requirement
Pitch-Roll Coupling (Frequency Domain)	S	Ensure pitch/roll decoupling
Min. Crossover Freq. (linear scale)	S	Ensure acceptable crossover
Dist. Rej. Bandwidth (Pitch)	S	Ensure Dist. Rej. Bandwidth
Dist. Rej. Bandwidth (Roll)	S	Ensure Dist. Rej. Bandwidth
Dist. Rej. Bandwidth (Yaw)	S	Ensure Dist. Rej. Bandwidth
Dist. Rej. Peak	S	Ensure good damping of disturbance response
Heave Response Hover/Low-Speed	S	Ensure good heave dynamics
Crossover Freq. (linear scale)	J	Over design
Actuator RMS	J	Over design

The optimization requirements are the HQ specifications mostly defined by ADS-33. Extra requirements about robustness issues and stability margins for rigid body frequency range are taken from GARTEUR and Mill-DTL-9490E respectively. All these requirements are build-in options of CONDUIT<sup>®</sup>, available to the user. The scope of ADS-33 covers the effects of degraded visual environments(DVE). Required agility and required response types are a function of applicable mission task elements(MTE) and usable cue environments(UCE) respectively. All these constrains form a quantitative criteria in frequency and time domain and qualitative criteria related to pilot ratings<sup>[12]</sup>. It falls upon to the flight dynamics engineer to select the feasible specifications for the problem at hand to come up with a sensible HQ evaluation. The selected specifications for hovering flight are in table 1. Each specification is assigned a type as hard constraint (H), soft constrained (S) or summed objective (J). The types of the constraints reflects their priority during optimization. Hard constraints has the highest priority, whereas the summed objective type has the lowest. The comment column of table 1 illustrates each specification's objective in terms of HQs.

The optimization algorithm computes new design parameters for each step, which becomes the weighing matrix elements for the linear quadratic regulator problem to

use. Controller gain matrices for the new weighing matrices are computed using optimal control theory and closed loop performance is checked against the selected HQ specifications. The iteration process continues until all the specifications are satisfied or better specification ratings are not possible. Defining the initial design parameters is a crucial choice, since all optimization history depends on the initial values of the design parameters. Time response analyses with the nonlinear model of the helicopter are performed to find the initial weightings by trial-and-error. Although the initial weightings failed to achieve Level 1 HQ ratings for any of the controllers, they proved to be adequate starting points for the optimization process.

## 5 HQ EVALUATION

The controllers' performance in terms of HQ are assessed after the optimization process is complete. Overall HQ rating for all of the controllers reflect Level 1 after the weighing optimization. However, tracking performance degraded considerably due to handling quality trade-off.

To increase traceability each specification plot is illustrated with all the controllers' results. In the below figures upper triangles represent pitch channel, lower triangles represent roll channel and the diamond shapes represent the yaw channel results. The coloring indicates the controller type: yellow is for RFF, white is for CGT, green is for IMF and cyan is used for MI controller. In the following subsections results are presented.

### 5.1 Tracking Performance

Since the LQR cost function is defined in the time domain for all the controllers, optimal closed loop gains main objective is to minimize the time domain tracking error. Titchler presents a method which makes quantifying the time domain tracking error in the form of a tracking cost possible<sup>[13]</sup>. The tracking cost is given by equation 31.

$$(31) \quad J_{rms} = \sqrt{\frac{1}{n_0 n_t} \sum_{i=1}^{n_t} [y_{ref} - y]^T W [y_{ref} - y]}$$

The  $y$  is the vector containing response of the closed loop system states that are selected as system performance outputs in equation 2. For each closed loop system, doublet inputs are introduced to each channel and nonlinear simulations were performed to quantify tracking errors. The tracking error results are tabulated in table 2.

Table 2: Tracking Cost - Nonlinear Results

Axis	CGT	RFF	IMF	MI
$\theta$	0.1640	0.2552	0.2252	0.3308
$\phi$	0.1772	0.2352	1.4307	0.7353
$w$	0.8502	0.1665	0.0760	0.1161
$\psi$	0.3126	0.2219	0.1177	0.1345
<b>Total</b>	<b>1.5040</b>	<b>0.8788</b>	<b>1.8496</b>	<b>1.3167</b>

$J_{rms} < 1$  to 2 indicates excellent to good tracking performance respectively. Excellent performance tracking is achieved for all controllers except in IMF  $\phi$  channel. The RFF controller exhibits the best overall performance with the lowest cost values in nearly all channels. All controllers present suitable tracking performance with the nonlinear model according to the tracking metric. Figure 4 illustrates the on axis tracking performance to a  $\theta$  command. Although, overall tracking performance metric is suitable, the on axis tracking seems poor except for CGT controller. Since the linear quadratic optimization cost function defined in time domain and the HQ specifications are selected in frequency domain, optimization effort degrades the tracking performance. This was an expected worsening and it is valuable to know that CGT architecture is robust enough to withstand this degradation.

### 5.2 Stability

The stability metrics are defined as hard constraints to ensure a stable closed loop under any weighing parameters selected. The optimization direction evolves in such a way that no hard constraint is ever violated. Even the optimal control theory ensures stability, a positive eigenvalue or a negative damping ratio was possible due to actuator/sensor dynamics or computational delays.

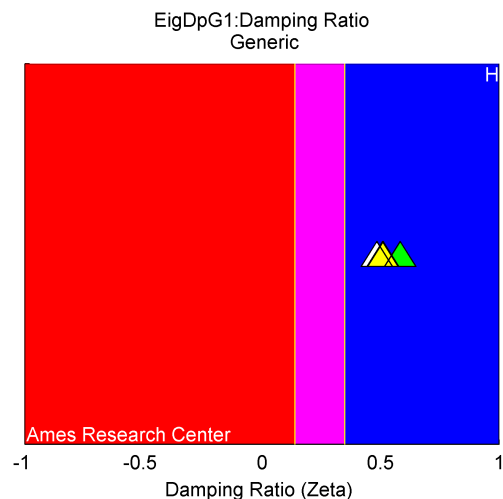


Figure 5: Damping ratio, all axes

Figure 5 illustrates the worst damping ratios for all controllers. Damping results shows the perfect model following

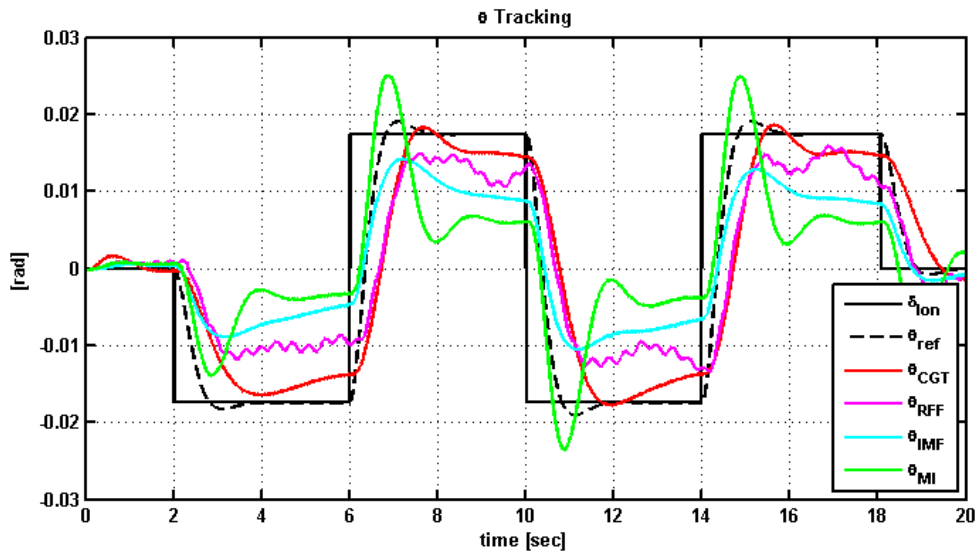


Figure 4:  $\theta$  tracking simulation

can not be achieved, since the reference model damping ratios were defined as 0.7 for pitch, roll and yaw channels. Still, the damping ratio metric shows Level 1 ratings for all controllers.

### 5.3 Robustness

Broken loop gain margin and phase margin of a closed loop system can be used as a measure of robustness. Figure 6 reflects the robustness of the individual channels of the controllers in the rigid body frequency range. The PM of the controllers range from 60 to 45 degrees. Yaw channels seem to have higher PM than the remaining axes for all controllers.

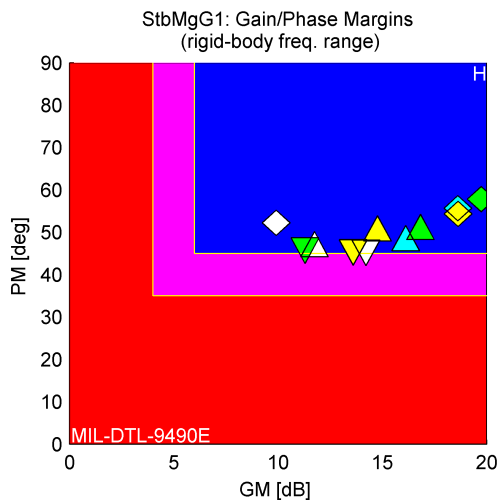


Figure 6: Gain-Phase margins

The only controller that has a low PM in both pitch and roll channels is CGT. GM values range considerable from 10 to 20 dB. None of the controllers seem too close to the GM

boundary for Level 1 HQ ratings. The same robustness characteristic is observed in the Nichols stability metric developed by GARTEUR.

### 5.4 Bandwidth and Crossover Frequency

Piloted bandwidth metrics are a good measure if the closed loop systems is prone to pilot-induced-oscillations or not. IMF has the best overall bandwidth in pitch and roll axes; where as, the CGT has the overall worst. The good IMF metric is understandable since the IMF tries to minimize the distance between the closed loop pole location with the reference models roots.

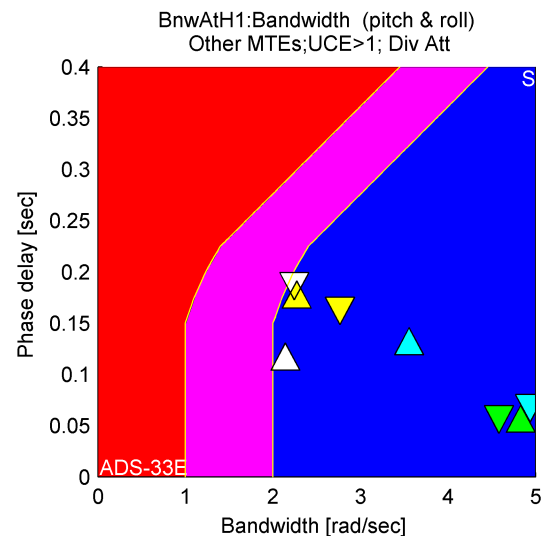


Figure 7: Pitch & Roll bandwidth

The explicit model following controllers have the reference model nested in their control algorithm. The reference signals need to pass through the reference model first. This

fact introduces an additive phase delay to the overall closed loop system as can be seen from Figures 7 and 8. RFF and CGT controllers have more phase delay than the IMF which naturally has less phase delay, and the MI controller. The MI controller is able to gain back some amount of phase by the inherent inversion in its control algorithm. For the pitch axis, the pseudo inverse does not cancel out the open loop dynamics completely, resulting in a lower bandwidth and higher phase delay than roll channel. The same inversion inadequacy is evident in Figure 8 for yaw channel.

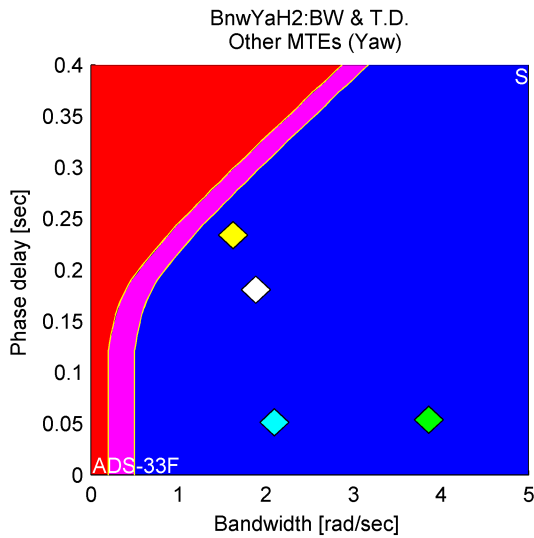


Figure 8: Yaw bandwidth

Figure 9 depicts broken loop crossover frequency values appropriately lie between limits of 2-10 rad/s. Pitch channel of the CGT has the highest crossover frequency which can corrupt the disturbance rejection performance.

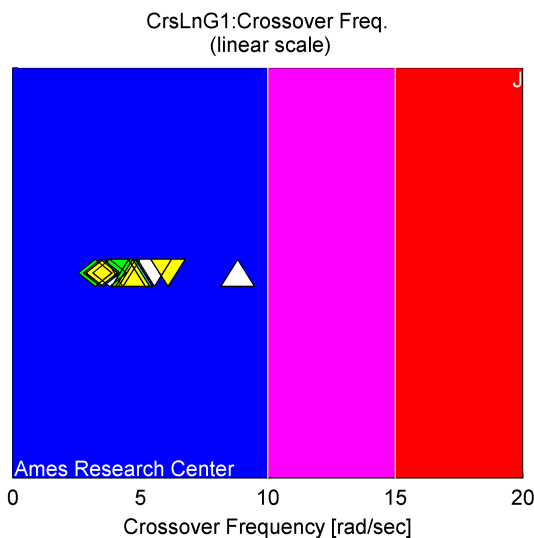


Figure 9: Crossover frequency

## 5.5 Pitch Roll Coupling

Figure 10 shows the coupling from pitch to roll and roll to pitch channels. All explicit model following controllers manage to have Level 1 ratings in terms of pitch roll coupling. On the other hand, IMF controllers shows Level 2 behavior. The extensive effort to achieve Level 1 coupling for IMF controller failed inescapably. Encapsulating reference model in the control law block diagram may cost extra phase delay or result in low bandwidth but in terms of decoupling performance, it proves to be invaluable. Although IMF controller has sufficient phase margin, changing weightings can not be used to decouple pitch and roll furthermore. Among the explicit model following controllers CGT has the lowest coupling from pitch and roll channels and MI has the lowest coupling from roll to pitch.

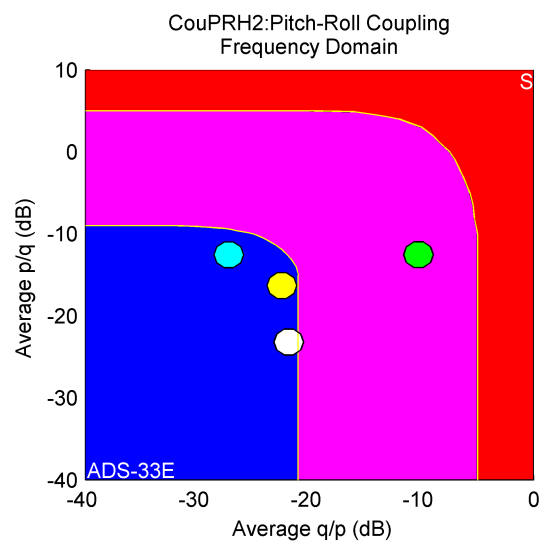


Figure 10: Pitch-Roll coupling

## 5.6 Disturbance Rejection

According to Blanken, "Experience has shown that a feedback system with adequate disturbance rejection bandwidth is recognized by the pilot as having good trimmability". Since good disturbance rejection performance is a must for state of the art controller design, disturbance rejection bandwidth criteria is included into the optimization problem as a soft constraint. For ACAH response types the disturbance rejection bandwidth is computed as the frequency where the bode magnitude curve for response to disturbance injected on to the related attitude feedback signal crosses -3 dB. It characterizes the speed of response recovery from a disturbance<sup>[12]</sup>. All disturbance rejection criteria exhibits Level 1 ratings.

Pitch channel of CGT controller has the least disturbance rejection bandwidth compared to the other controllers which is an expected outcome as indicated by crossover frequency values.

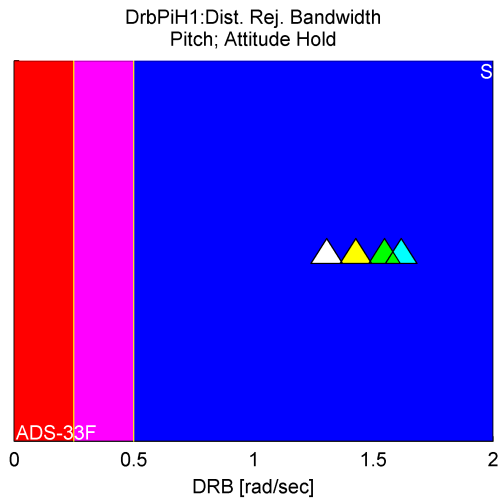


Figure 11:  $\theta$  disturbance rejection bandwidth

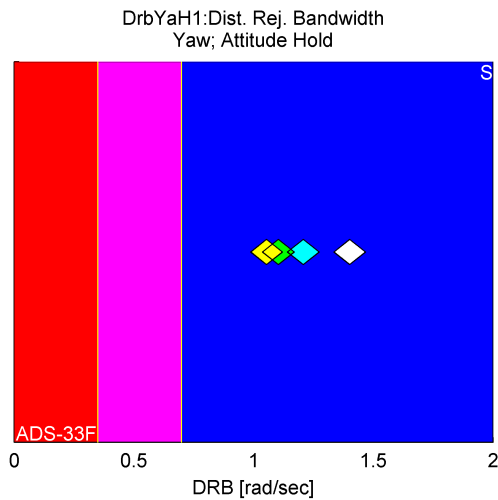


Figure 12:  $\psi$  disturbance rejection bandwidth

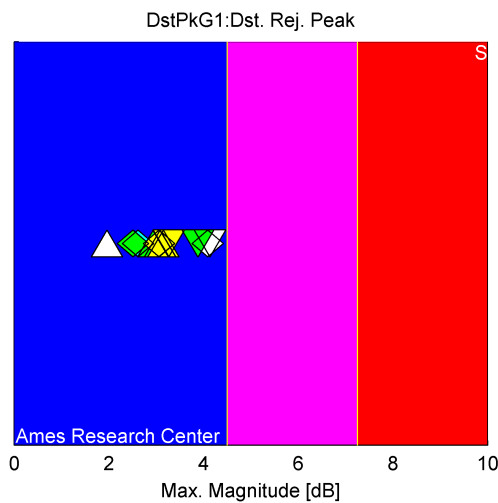


Figure 13: Disturbance rejection peak, all axes

Roll channel values are well above Level 1 boundary.

The bandwidth values are all above 2 rad/s, except for CGT controller, which has a 1.5 rad/s disturbance rejection bandwidth.

CGT has the highest disturbance rejection bandwidth on the yaw channel. All other controllers have similar bandwidths. Disturbance rejection bandwidth is inversely proportional to disturbance rejection peak for most of the controllers, CGT being the most obvious one.

### 5.7 Heave Response

The vertical rate response has a qualitative first order appearance for at least 5 seconds following a step as desired by ADS-33E-PRF. It is uncommon for a helicopter to disobey this requirement. As can be seen from Figure 14, all controllers satisfy Level 1 heave response criteria. CGT controller shows the highest heave mode frequency, indicating a delayed tracking with a low steady state error.

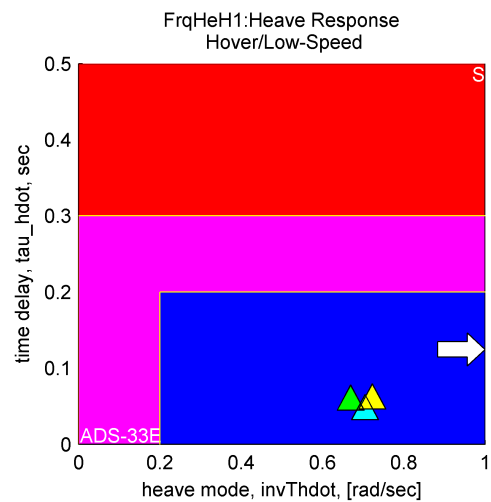


Figure 14: Heave response

### 5.8 Actuator Usage

Actuator usage specification measures the RMS actuator position which is found by using the area under the output autospectrum. It is included in to the optimization process as a summed objective constraint. Actuator usage of the IMF controller for the pitch and yaw channels close to Level 1 boundary, which makes IMF more prone to actuator position or rate saturation among all the controllers. This phenomena can further be investigated via Lateral Reposition and Acceleration/Deceleration MTEs as recommended by test guide<sup>[14]</sup>. IMF controller is followed by MI controller. The CGT and RFF controllers exhibit decent actuator usage.

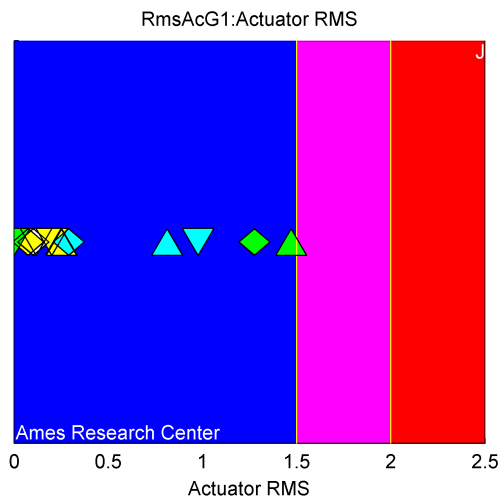


Figure 15: Actuator RMS, all axes

## 6 CONCLUSIONS

In this work four different types of model following controllers are designed for hovering flight of a teetering rotor helicopter. The controllers use optimal control theory, which minimizes a time domain cost function. Initial weightings which shows good tracking of the reference model are selected by trial-and-error with the help of nonlinear simulations.

CONDUIT<sup>®</sup> is a powerful tool for frequency domain based optimization. An optimization effort was carried out using the hover and low speed specifications for the designed flight controllers. The diagonal elements of the weighing matrices are used as design parameters during optimization. Forcing controllers to acquire Level 1 frequency domain specifications, degraded the preciously achieved time domain tracking performance. An obvious trade-off between the frequency and time domain requirements is evident from the results. For better time domain tracking performance without losing performance in the frequency domain, one can include of non-diagonal weighing matrix elements as design parameters to the optimization problem to provide the optimization algorithm more flexibility.

Level 1 response criterion are satisfied for the selected specifications except for the pitch/roll coupling specification of the IMF controller. All controllers are evaluated in terms of stability, damping ratio, robustness, coupling, bandwidth and heave response. The performances of the controller's are assessed in an effort to identify the drawbacks and strengths of a particular method originating purely by the controller synthesis.

Although the time domain tracking results are discouraging, the frequency domain specifications are promising. A balance between the tracking and handling qualities requirements can be found. Only then, frequency domain performance for the other flight conditions than hover will

be checked by using forward flight specifications to be able to perform piloted simulations.

## References

- [1] Mark B Tischler, Christina M Ivler, M Hossein Mansur, Kenny K Cheung, Tom Berger, and Marcos Berrios. Handling-qualities optimization and trade-offs in rotorcraft flight control design. In *AHS Specialists Meeting on Rotorcraft Handling-Qualities, Liverpool, UK*, pages 4–6, 2008.
- [2] Gareth D Padfield. Rotorcraft handling qualities engineering: Managing the tension between safety and performance 32nd alexander a. nikolsky honorary lecture. *Journal of the American Helicopter Society*, 58(1):1–27, 2013.
- [3] Brian L Stevens and Frank L Lewis. *Aircraft control and simulation*. John Wiley & Sons, 2003.
- [4] Christopher Adams, James Potter, and William Singhose. Input-shaping and model-following control of a helicopter carrying a suspended load. *Journal of Guidance, Control, and Dynamics*, 38(1):94–105, 2014.
- [5] MJ Spires and JF Horn. Multi-input multi-output model-following control design methods for rotorcraft. American Helicopter Society, Inc, 2015.
- [6] MJ Spires and Horn JF. Multi-input multi-output model-following control design methods for rotorcraft. In *Annual Forum Proceedings-American Helicopter Society*. American Helicopter Society, 2015.
- [7] Michael Trentini and Jeff K Pieper. Model-following control of a helicopter in hover. In *Control Applications, 1996., Proceedings of the 1996 IEEE International Conference on*, pages 7–12. IEEE, 1996.
- [8] Anon. Aeronautical design standard, handling quality requirements for military rotorcraft, ads-33e-prf. U.S. Army Aviation and Missile Command (USAAMCOM), 2000.
- [9] He Chengjian. Flightlab theory manual. *Mountain View CA: Advanced Rotor Craft Technology Inc*, 2004.
- [10] JS Tyler Jr. The characteristics of model-following systems as synthesized by optimal control. *Automatic Control, IEEE Transactions on*, 9(4):485–498, 1964.
- [11] Eliezer Kreindler and David Rothschild. Model-following in linear-quadratic optimization. *AIAA Journal*, 14(7):835–842, 1976.
- [12] CL Blanken, MB Tischler, JA Lusardi, and CM Ivler. Aeronautical design standard-33 (ads-33) past, present, and future. In *AHS Rotorcraft Handling Qualities Specialists Meeting, Huntsville, AL*, 2014.
- [13] Mark B Tischler and Robert K Remple. Aircraft and rotorcraft system identification. *AIAA education series*, 2006.
- [14] Chris L Blanken, Roger H Hoh, David G Mitchell, and David L Key. Test guide for ads-33e-prf. Technical report, HOH AERONAUTICS INC LOMITA CA, 2008.